Measurement 236 (2024) 115096

Contents lists available at ScienceDirect

Measurement

journal homepage: www.elsevier.com/locate/measurement

Non-destructive vibration-based monitoring analysis of PV modules with encapsulant degradation by frequency change

Chiara Bedon *, Alessandro Massi Pavan

University of Trieste, Department of Engineering and Architecture & Center for Energy, Environment and Transport Giacomo Ciamician, Trieste, Italy

ARTICLE INFO

Keywords:
photovoltaic (PV) modules
Mechanical properties
Materials
Experiments
Numerical modelling
Vibration frequency

ABSTRACT

In engineering applications, the frequency analysis represents a first and practical step to collect relevant parameters for structural and mechanical diagnostics. Any possible material / component degradation and deterioration can be prematurely detected by frequency modifications that exceed a certain alert value. In this paper, the attention is given to the dynamic mechanical analysis of commercial photovoltaic (PV) modules, in which the solar cells are typically encapsulated in thin viscoelastic interlayers made of Ethylene-Vinyl Acetate (EVA), which are primarily responsible for the load-bearing capacity of the sandwich PV system. As a major effect of ageing, ambient conditions, non-uniform / cyclic thermal gradients, humidity and even extreme mechanical / thermal loads, the rigidity of these films can largely modify and decrease, thus possibly affecting the mechanical capacity of the PV module, and even exposing the solar cells to fault. Knowledge of the effective bonding level is an important step for diagnostic purposes. In this regard, the present study is based on a preliminary non-destructive experimental analysis, and on an extensive parametric Finite Element (FE) numerical investigation of full-scale commercial PV modules of typical use in buildings. The attention is given – for PV module arrangements of technical interest – to the effect of EVA stiffness in terms of vibration modes and frequency sensitivity. As shown, especially compared to newly installed PV modules, any kind of stiffness decrease is associated to major frequency modifications for the composite system, and in the worst configuration, such a frequency scatter can decrease down to −40% the original condition. Such a marked stiffness decrease would be implicitly associated to a weak mechanical performance of the sandwich section, with major stress peaks and deflections in the PV system, even under ordinary loads. The presented results, in this sense, suggest that major consequences can be prevented and minimized by monitoring the vibration frequency of PV modules.

1. Introduction

Photovoltaic (PV) modules are designed to ensure more than 25 years of functionality under variable and even unfavourable operational conditions, including the effect of temperature / humidity changes, wind, rain, hail and snow, etc. While their electrical functionality is of primary importance, the mechanical performance also represents a critical aspect, which is implicitly correlated to the durability and efficiency of PV modules. According to literature, in this regard, there are several monitoring and diagnostic strategies to monitor possible faults and defects, such as shading, dust or sand accumulation on the PV surfaces, short circuits, bypass diodes failures, disconnections of PV modules, shunting of PV modules, and others [1–3]. Hot spot faults represent one of typical localized damage configurations that should be promptly detected [4–7].

Structurally speaking, a special care should be required for the prompt detection of many different progressive degradation / failure mechanisms that are associated to possible power-losses and major effects on the functionality and efficiency of PV modules, such as possible micro and macro cracks in cells [8], breakage of interconnects [9], detachment of the frame members at the edges, and especially delamination of sandwich components in the PV system [10–13].

As in Fig. 1, the majority of commercial PV modules are in fact usually characterized by a relatively thin cross-section and a typically high slenderness and bending flexibility to out-of-plane mechanical loads, due to their size-to-thickness ratio and also to the typical arrangement of restraints and fixings. As a sandwich cross-section, the mechanical capacity is mostly assigned to thin glass covers with typical thickness in the range $h_1 \approx$ 3–5 mm and (for single-glass compositions) back Tedlar® / plastic layers ($h_2 \approx$1-2 mm), which are mechanically

* Corresponding author at: Via Valerio 6/1, 34127 Trieste, Italy.
E-mail address: chiara.bedon@dia.units.it (C. Bedon).

https://doi.org/10.1016/j.measurement.2024.115096
Received 1 December 2023; Received in revised form 21 May 2024; Accepted 8 June 2024
Available online 10 June 2024

bonded by Ethylene-Vinyl Acetate (EVA) interlayers with $h_{int} \approx 1$ mm in total.

For a system like in Fig. 1, there are several influencing parameters to properly take into account for structural / mechanical considerations and diagnostics.

Regarding the environment effects, for example, chemical additives in use to retard possible deterioration of EVA layers, according to literature, can indeed also contribute in anticipating the degradation of adhesion strength [13]. Also, PV modules are designed to ensure functionality in a temperature range from −40° to + 85 °C, which represents a major thermal gradient exposure for the sandwich components. Considering that the temperature distribution in PV modules is typically non-uniform and largely depends on the geometry and the materials in use [14–17], such an operational condition can involve further sensitivity and possible non-uniform degradation of the encapsulant stiffness / adhesion. To assess these aspects, many studies have been dedicated to the experimental and numerical analysis of PV modules under different mechanical loads, including the effect of ordinary pressures for different boundary conditions [18,19] and even impact or hailstorm events [20,21]. In most of cases, specific modelling strategies are taken into account to explore quasi-static or dynamic load-bearing behaviours and mechanisms [22,23]. As known, however, most of mechanical (and thus functional) issues can also derive from the geometrical features of commercial PV modules [24].

The interposed thin films in Fig. 1 are used to encapsulate and protect the solar cells, and to ensure the shear bond of external covers. As such, they have a primary role in the determination of the mechanical and load-bearing capacity of the PV module as a whole. Besides, as it is for most of laminated glass applications for constructions, EVA films are characterized by a typical non-linear viscoelastic behaviour [25–29] and a generally low stiffness, compared to the front/back covers. Specific mathematical models should be thus taken into account for mechanical considerations on PV modules [30]. Assured that there are many different ageing effects on EVA foils, and the use of various additives can only in part mitigate these phenomena [13,31], it was observed by many experimental / numerical mechanical studies (see for example Fig. 2 (a) and (b)) that the stress distribution in the thickness of the sandwich components for PV samples under quasi-static uniform pressure is largely affected by the presence of a relatively soft core, even under optimal environment conditions.

Also, the experimental studies reported in [25–29] emphasized the effects of ageing and unfavourable outdoor conditions on the mechanical properties (i.e., rigidity) and failure modes of the material itself, compared to other typical interlayers in use for laminated glass. The parametric analysis presented in [32] highlighted the effects of thermo-mechanical loads and thickness details on the stress and deflection performance of commercial PV modules. The research studies presented in [33,34] focused on the rheological characterization, by Maxwel model and Prony series or fractional calculus, of the non-linear viscoelastic behaviour of EVA encapsulants (Fig. 2 (c) and (d)), pointing out the associated effects under typical thermo-mechanical operational conditions for PV modules. The minimum shear bond required to satisfy mechanical performances was investigated in [35].

Following the above considerations and the existing literature evidences, an experimental and Finite Element (FE) numerical study is thus presented in this paper to assess the convenience of non-destructive dynamic techniques for the mechanical characterization and for the early damage / deterioration detection of EVA bonding interlayers for PV modules (Fig. 3). The methodology takes advantage of classical structural health monitoring (SHM) procedures for civil structures and machineries [36–38], where the on-site experimental analysis in the frequency domain is carried out to detect and characterize the vibration modes of the system object of study, and thus to assess the effect of single components and possible influencing parameters. The approach follows earlier applications to laminated glass systems and composite elements, where in-field and/or historic structures have been efficiently

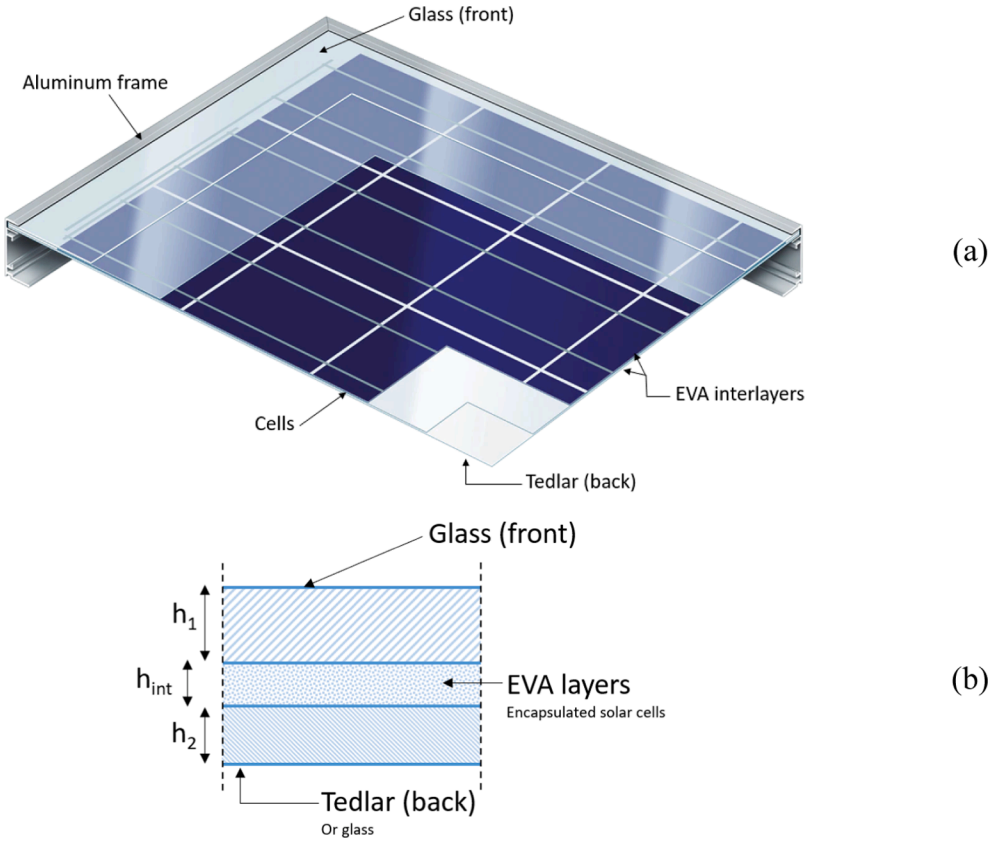

Fig. 1. Reference commercial PV module (example): (a) axonometry and (b) schematic cross-section.

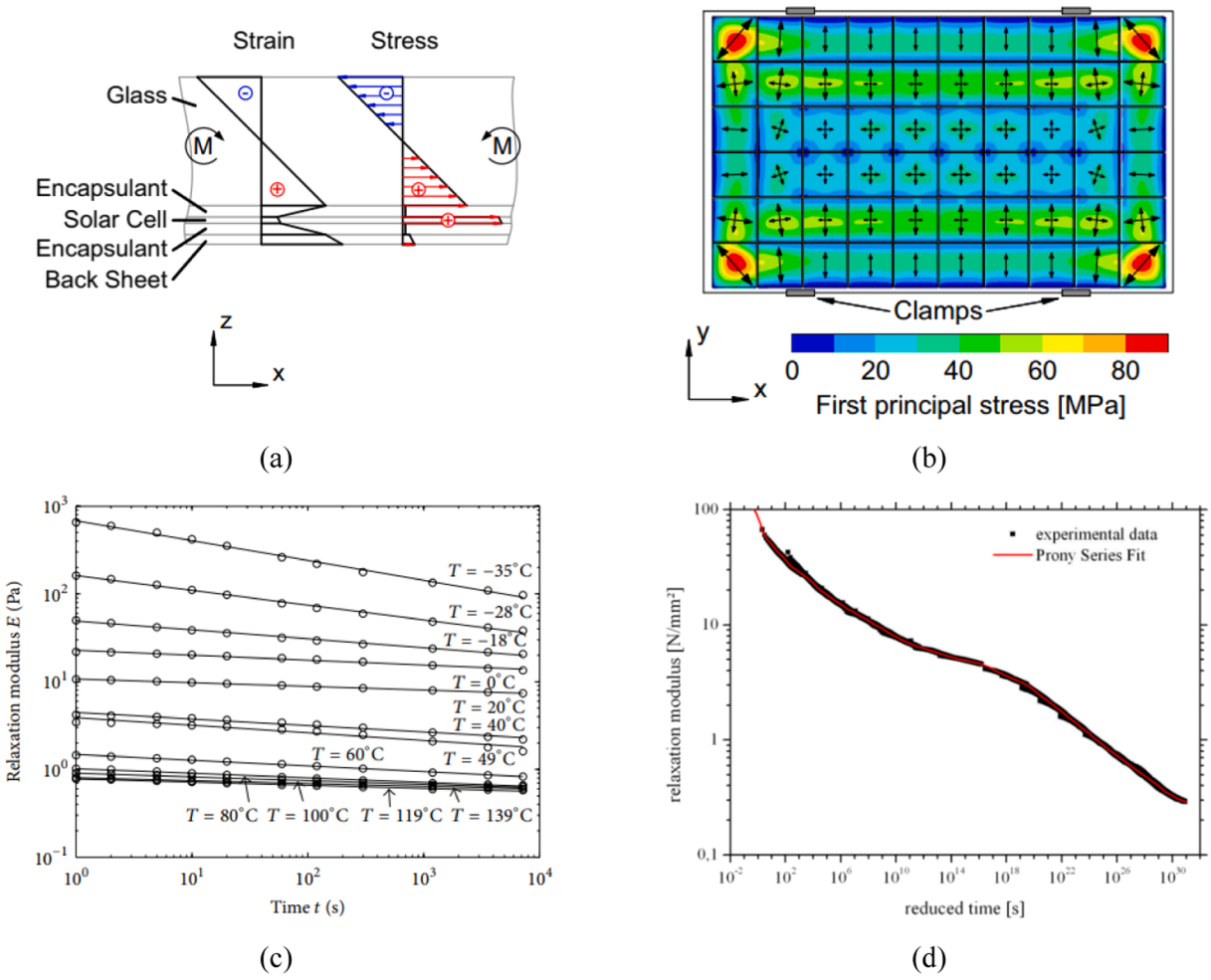

Fig. 2. Example of stress analysis in a PV module under mechanical out-of-plane loading: (a) cross-section and (b) front view (reproduced from [8] with permission from Elsevier©, copyright license number 5654100960128, October 2023); (c)-(d) examples of experimentally derived relaxation modulus for EVA encapsulants, as a function of time and temperature (reproduced from [33,34] under the terms and conditions of a CC-BY license agreement).

characterized under various loading and boundary conditions, including walkways in unfavourable environment and operational configurations [39], historic facades [40], fractured pedestrian systems [41], structural beams with delamination [42], and even film-retrofitted glass members investigated under severe post-fracture configurations [43,44].

The present study indeed consists, differing from [39–44], in the analysis of composite systems characterized by higher flexibility (due to typical geometrical and mechanical features), severe exposure to environment, and thus higher sensitivity to possible material degradation. To this aim, non-destructive experiments are performed on a selection of commercial PV modules, with a major attention for the low vibration modes and corresponding frequencies. The experimental frequency analysis described in Section 3, more in detail, is used to support the definition and calibration of a FE numerical model representative of the reference PV module, in which the basic constituent members are efficiently described in geometrical and mechanical terms, and the EVA material is described as equivalent liner elastic (Section 4). Verified that the assembled FE model is able to rather well capture and reproduce the dynamic features of a newly assembled PV module, parametric numerical analyses are carried out in Section 5 to address the sensitivity of dynamic features to basic material modifications for the bonding encapsulant, which could take place due to progressive ageing in the long-term period, exposure to unfavourable ambient conditions, repeated thermal gradients, and even possible localized / non-uniform delamination or damage due to extreme mechanical loads.

2. Background

For the present investigation, due to the availability of full-scale samples to test before their final installation on a roof, a set of single-glass PV modules like in Fig. 1 (a) were taken into account. The typical system in Fig. 1, in particular, it characterized by maximum dimensions $H = 1.75$ m in height $\times$ $B = 1.15$ m in width, with a total weight of about $W \approx 21$ kg. The sandwich section is composed of a tempered glass cover on top ($h_1 = 3.2$ mm), a Tedlar cover on the back ($h_2 = 1$ mm) and two interposed EVA layers ($h_{int} = 1$ mm in total) to embed the solar cells. The supporting frame along the edges is made of anodized aluminium and is point-fixed to the substructure by four aluminium brackets. For practical convenience, the series of non-destructive experiments was carried out on a single typology of PV modules only. Besides, similar methodological considerations can be extended to double glass PV modules in which the back plastic layer is replaced by a glass panel.

The current approach assumes that the frequency analysis of PV modules – experimentally derived based on the Fourier Transform function analysis of measured acceleration records – can offer important feedback and can be used to calibrate and validate a refined FE model representative (in average) of the tested PV samples, in which the geometry and the mechanical composition of a selection of commercial full-scale modules is properly taken into account. Based on the experimental validation of the reference FE model described in Section 4, the numerical analysis is further extended to a parametric and sensitivity

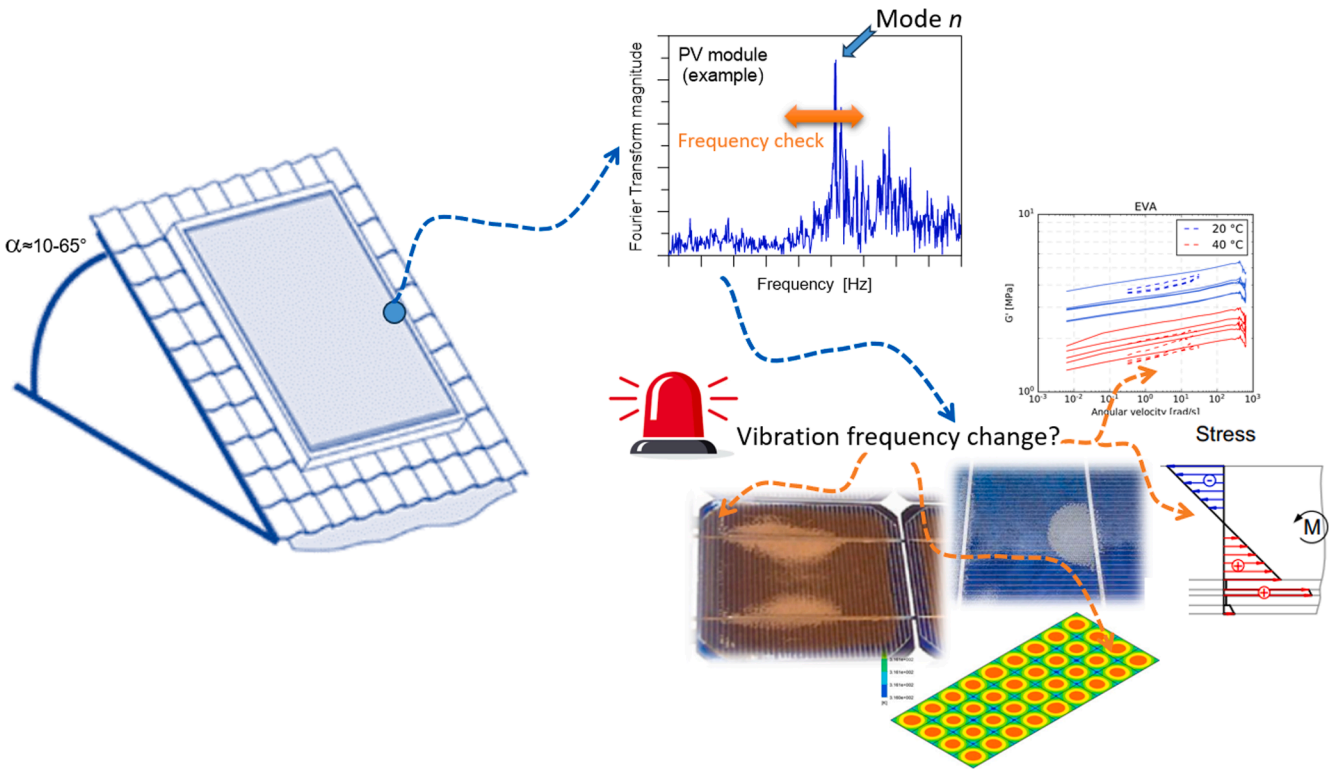

Fig. 3. Scheme of present methodology and investigation.

study, to assess the effect of further influencing parameters of technical interest for long-term and severe ambient conditions.

Under unfavourable environments, the vibration frequency of the PV system in Fig. 4 (a) is in fact affected by many factors, that are namely associated to the sandwich section features (Fig. 3 (b)), to the contribution and edge restrain of the metal frame (Fig. 4 (c)), to the effect of brackets (Fig. 4 (d)), etc.

At the level of sandwich in Fig. 4 (b), the protective glass cover is expected to behave elastically without significant modifications in the elastic modulus of the basic constituent material [45], and the same concept applies to the aluminium components of frame members and restraints. Besides, the interposed EVA films are sensitive to temperature and humidity, which could both affect the PV modules in the long-term period [32,46]. As far as the bonding interface of EVA films and glass/plastic covers is possibly affected by external agents, and/or the interlayer suffers for stiffness modification due to operational conditions, the PV module acts as a composite panel with weak / flexible shear connection, and this could result in compromised load-bearing mechanisms under design mechanical loads [30,47].

On the other side, it is experimentally proved that high vibration frequencies for EVA films – like for viscoelastic interlayers in general – typically have a stiffening effect, and this can be positively quantified in a possible moderate increase in shear bond efficiency [29,46]. However, it is also experimentally observed that repeated mechanical loads (even at high strain rate) induce a marked reduction in the material stiffness, with deterioration of shear bond rigidity [48]. In such a variable and

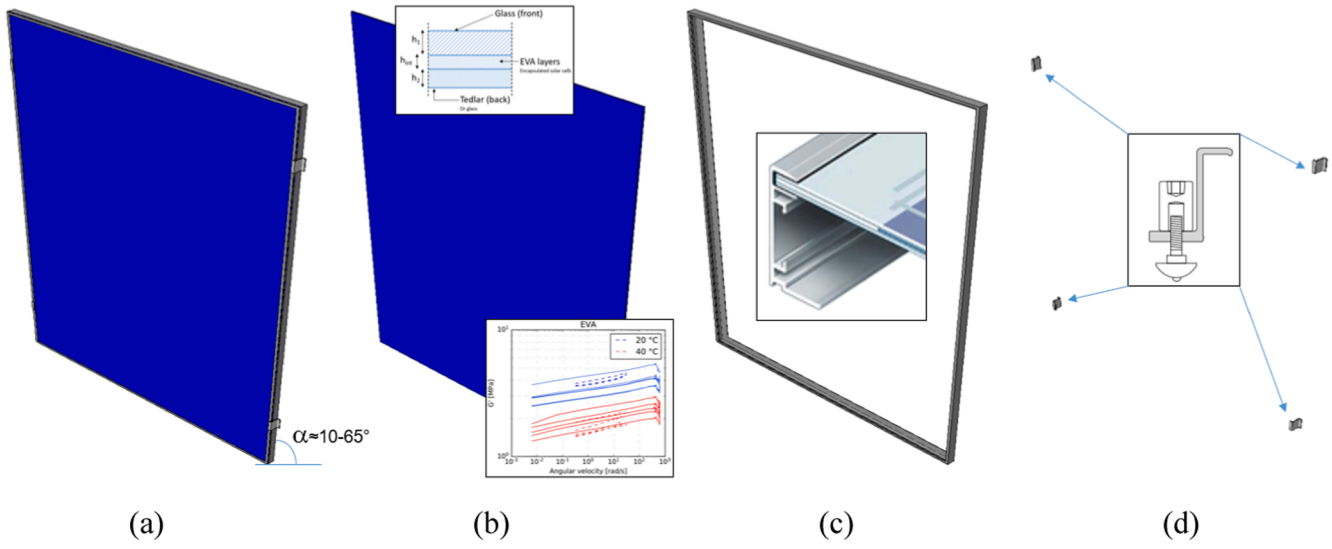

Fig. 4. Influencing parameters in the frequency analysis of a PV module: (a) reference system, (b) sandwich panel, (c) frame, (d) brackets.

uncertain scenario, both the metal frame at the edges (Fig. 4 (c)) and the fixing brackets (Fig. 4 (d)) – that can be efficiently characterized by numerical analysis – further contribute to modify the vibration response of the PV system, compared to ideal simplified restraints.

To assess the severity of all these possible effects, the present study assumes that – for the sandwich section – the stiffness of EVA films and its viscoelastic modification are for the major part responsible of the vibration frequency and rigidity of a given PV module in out-of-plane bending deformations. The "effective" composite flexural stiffness of the sandwich is in fact [18,47,49]:

$$D_{eff} \approx f(glass, EVA, Tedlar) \tag{1}$$

Rationally, it is expected that:

$$D_{abs} \le D_{eff} \le D_{full} \tag{2}$$

where D_{abs} and D_{full} denote the bending stiffness values of the sandwich section under weak / null shear bonding offered by EVA foils ("abs", layered limit) or with ideally rigid connection in shear ("full", monolithic limit) respectively.

From an analytical point of view, as also in accordance with [18] and other studies, the basic assumption for the analytical mechanical analysis of a sandwich section like in Fig. 4 (b) is that:

- the front glass cover (h_1 thickness) is described as linear elastic layer (with E_1, ν_1, ρ_1 the material properties in terms of modulus of elasticity, Poisson' ratio, density);
- the backboard Tedlar layer (h_2 thickness) can be also described as linear elastic (E_2, ν_2, ρ_2);
- the EVA interlayer, with total thickness h_{int}, is described as an equivalent linear elastic material with secant stiffness E_{int} which is in general very soft compared to E_1 and E_2. For more realistic estimates, however, this value should be calibrated to represent – based on the typical viscoelastic material behaviour – a specific loading and boundary condition of practical interest (i.e., time loading, temperature, ageing [49]);
- the encapsulated solar cells are disregarded in mechanical terms, and assumed to offer null contribution to the composite PV section in bending.

Under such a kind of assumption, it is conservatively expected that the bending stiffness of the sandwich section is mostly governed by the front and back covers only, where ($i = 1, 2$):

$$D_i = \frac{E_i h_i^3}{12(1-\nu_i^2)} \tag{3}$$

is the stiffness of external layers and the limit values are:

$$D_{abs} = \sum D_i \tag{4}$$

$$D_{full} = D_{abs} + \frac{12 D_1 D_2}{D_1 h_2^2 + D_2 h_1^2} H^2 \tag{5}$$

with:

$$H = h_{int} + \frac{h_i}{2} \tag{6}$$

The corresponding deflection under uniform pressure and simple boundary conditions can be thus estimated analytically, see for example [30].

The fundamental vibration frequency f_1 of the sandwich system like in Fig. 4 (b) can be also roughly expressed – as far as the frame members at the edges are disregarded and the real restraints are described as ideal clamps or supports – by means of simplified analytical models of literature [50]. For ideal simply supports along the four edges, for example, it is:

$$f_1 = \frac{\omega_1}{2\pi} = \frac{\pi}{2}\left(\frac{1}{a^2} + \frac{1}{b^2}\right)\sqrt{\frac{\overline{D}}{\overline{m}}} \tag{7}$$

where $\overline{D} \neq D_{eff}$ is the actual bending stiffness of the system, and $\overline{m}$ is its weight per unit of area.

The present experimental and FE numerical study overcomes the intrinsic limits of Eq. (7) and explores different configurations of practical interest.

3. Background experimental methods

The experimental investigation was carried out on a selection of full-scale PV modules like in Fig. 5 (a)-(b), with a typical cross-section layout corresponding to the scheme in Fig. 1 (a). The experimental analysis was carried out in a beam-like setup for the PV modules of Fig. 5, that means samples with short edges simply supported and long edges fully unrestrained. A total of 5 samples was considered, under similar testing conditions. The vibration experiments followed a series of preliminary inspections on the PV modules, that were carried out to measure the relevant thicknesses and dimensions of interest for the description of FE model.

A single MEMS sensor was used for the analysis of typical PV module under low-amplitude, random excitation. During the experimental analysis, the sensor was rigidly bonded to the Tedlar layer of each sample, in the mid-span section. The use of a mini device like in Fig. 5 (c) was preferred to avoid the influence of mass and size of sensor on the bending response and dynamic parameters of the typical PV module. The MEMS device in use consisted in a wireless device based on IMU AHRS MPU6050 chip board, inclusive of a three-axes accelerometer sensor (±16 g its range, 0.005 g the resolution, 0.2–200 Hz the available sampling rate). The size of sensor (cover included) was measured in 36 × 36 mm, with 15 mm the thickness and 20 g the weight.

4. Numerical investigation

4.1. Model assembly

The reference FE model was assembled in ABAQUS [51]. To optimize the computational cost of simulations, the FE model consisted of a combination of full 3D solid brick elements (for the metal frame and brackets) and 2D shell elements for the PV components schematized in Fig. 1 (i.e., glass cover, EVA, Tedlar layer, solar cells). To account for possible complex vibration modes, the full geometry of PV modules like in Fig. 5 was numerically described. The adopted mesh pattern was chosen to ensure accuracy in frequency estimates, and thus resulted in ≈28,000 elements and ≈42,000 DOFs, see Fig. 6.

Materials were described in the form of linear elastic constitutive laws, for the purpose of linear modal analyses and frequency predictions. For glass and aluminium, the nominal mechanical properties in Table 1 were taken into account [52,53]. The Tedlar plastic layer was mechanically characterized based on product datasheets, see Table 1 and [54]. Finally, for the EVA interlayer, the tentative mechanical characterization was preliminary based on experimental and numerical studies reported in [18,29]. To note that in the present analysis, the solar cells were described as an equivalent linear elastic material [18].

4.2. Solving approach

Linear modal analyses were carried out on the reference model in Fig. 6 (b), and the lower vibration modes were predicted in terms of shape and frequency. For the comparative and validation analysis of the numerical, more in detail, the experimental frequency values from Section 3 were only taken into account as in the experimental setup.

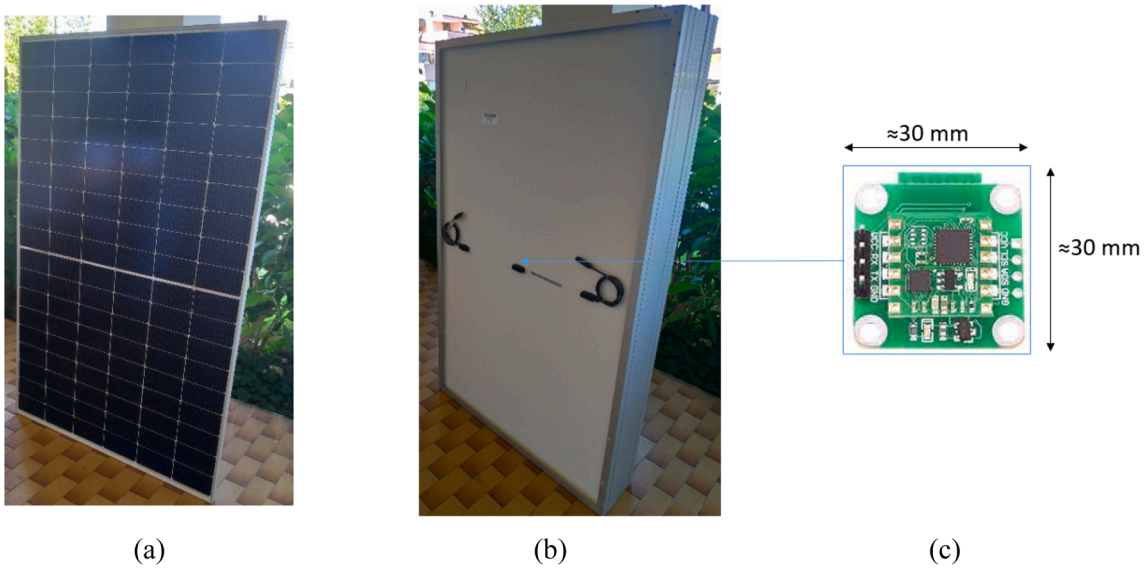

Fig. 5. (a) Front and (b) back view of selected PV modules (before testing), with (c) detail of MEMS sensor (out-of-scale).

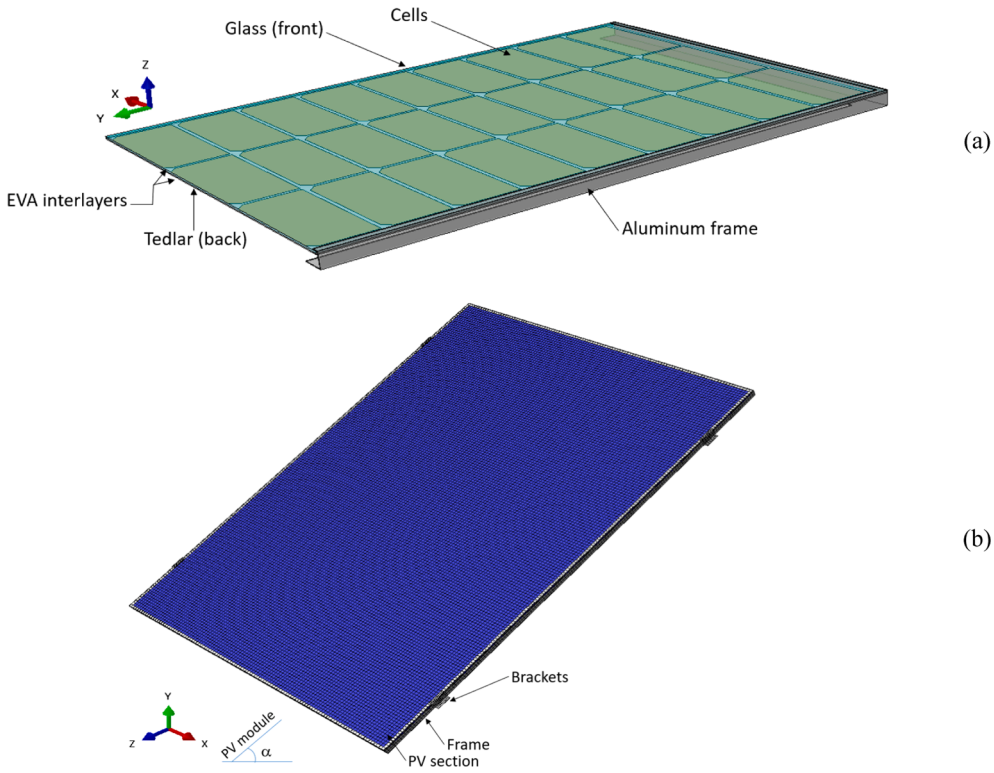

Fig. 6. Numerical model (ABAQUS): (a) assembly concept (1/4th geometry with symmetry boundaries) and (b) example of axonometric view for the PV module with mounting system ($\alpha = 40°$).

Table 1
Input mechanical properties for the frequency analysis (ABAQUS).

		Glass	Aluminium	Tedlar	EVA	Solar cells
E	[GPa]	70	69	25	0.005	170
ν	–	0.23	0.3	0.3	0.49	0.25
ρ	[kg/m^3]	2490	2700	1000	950	2330

Successively, the FE model was rearranged in inclined positions (with four metal brackets included), like in Fig. 6 (b), and subjected to further parametric simulations.

In both the circumstances, the FE assembly was investigated in two subsequent steps. First, a quasi-static geometrical nonlinear step was run to linearly impose gravity loads to the model components. Afterwards, the linear modal analysis as carried out on the pre-loaded FE model.

The parametric analysis was successively carried out by taking into account possible modifications in the equivalent secant modulus of EVA films, in terms of vibration frequency sensitivity and modal shape adjustment for the lower modes of the system.

4.3. Quasi-static considerations

There are no doubts that the progressive modification of interlayer stiffness (both for mechanical deterioration or delamination issues) should be possibly monitored because of its major effects on the load-bearing capacity of the sandwich section in PV modules. To highlight further such a possible condition, a selection of preliminary numerical results is presented in Fig. 7 for the PV module under a uniformly distributed quasi-static pressure q. To better quantify possible local effects and relative sliding of sandwich components, the analysis was carried out on a full 3D solid FE model reproduced in Abaqus according to Section 4.1. The high computational cost of analysis, as a consequence of the use of full 3D solid elements for all the PV components (43,000 elements and 220,000 DOFs), was compensated by the description of 1/4th only of PV module geometry with brackets (under appropriate symmetry conditions).

The selected numerical results in Fig. 7 (a) confirm, according to several literature studies [11,12,19,27], the critical role of interlayers in the quasi-static response to mechanical loads. Also, the presence of PV components and mounting details for the FE model in use can be perceived in the deformed shape of the system in Fig. 7 (b), which emphasizes the local effect of boundaries at the edges and supports. In this regard, the present study goes beyond the mechanical studies of literature, exploring the material deterioration in terms of frequency sensitivity and possible efficiency of non-destructive monitoring approaches.

5. Discussion of numerical results

5.1. Preliminary experimental and numerical assessment

The analysis was first focused on the numerical detection of lower vibration modes of the experimentally investigated PV modules. Typical results are reported in Figs. 8 and 9 in terms of vibration frequencies and shapes respectively. It can be noted that – for the four lower vibration modes of the experimental samples – there is in general a rather good correlation with the numerical evidences. The experimental frequencies derived from multiple measurements on PV samples resulted in a standard deviation around ± 0.6 Hz, with higher sensitivity for the second vibration frequency only (Fig. 8 (a)). Overall, the calculated percentage scatter for the numerical frequency predictions towards the average experimental estimates was quantified in about ± 2 % (Fig. 8 (b)).

More in detail, the fundamental vibration frequency was measured in f_1 = 10.63 Hz and 10.91 Hz respectively from experiments and numerical analysis, and corresponds to the flexural bending mode of the PV module with simply supports at the short edges only (Fig. 9 (a)). The subsequent vibration frequencies wee associated to the first torsional mode (Fig. 9 (b)) and to the higher flexural bending modes (Fig. 9 (c)-(e)) respectively.

5.2. Parametric numerical analysis

The numerical model validated in Section 5.1 was successively investigated under a practical configuration like in Fig. 6 (b), that is fixed by means of four metal brackets and supposed installed with a tilt angle α = 40°.

5.2.1. Mounting structure

As far as the supporting frame is restrained by the four brackets only, the typical vibration modes were found to largely modify compared to the experimental setup, in terms of bending deformation of the frame itself along both the long and short edges of the PV module. The typical vibration shapes are presented in Fig. 10.

Compared to Fig. 8, it can be noted – as expected – that the fundamental mode is still mostly associated to the first flexural bending deformation of the PV module. Also, the fundamental vibration mode is well separated by the other vibration modes of the system. Besides, differing from Fig. 8, the presence of lateral brackets to restrain the panel manifests in a lack of torsional vibration modes of the PV module, whose dynamic response in Fig. 10 is indeed characterized by the higher flexural bending modes of the point-fixed sandwich section, and by the partial flexibility of the supporting frame, hence resulting in an increasing number of half sinewaves.

5.2.2. Tilt angle

The PV module arrangement (i.e., frame, brackets features and position) has certainly direct effect on the local and global performance of the system. In term of vibration frequency, its sensitivity to PV module arrangement was also numerically explored for a set of practical configurations of technical interest. Assuming the material properties of Table 1 and the brackets positioned as in Fig. 6, more in detail, the tilt angle α of the module was progressively modified in a range of 10 to 70°. Major sensitivity was noticed by increasing α, as emphasized by the selection of results reported in Fig. 11. The effect of superimposed self-weight of PV module components with the geometrical properties of the system and the shear efficiency of the interlayer bond is in fact summarized. Numerical results are presented in Fig. 11 (a) in terms of average frequency by varying α, and confirm a minimum effect of tilt angle in terms of dynamic parameters of the PV system. For the PV module with material properties like in Table 1, the scatter of predicted

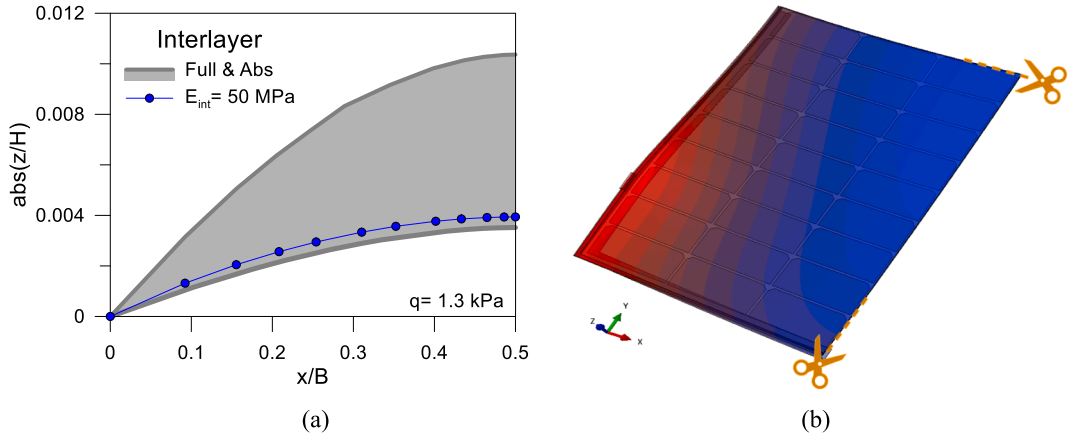

Fig. 7. PV module under uniform pressure q = 1.3 kPa: (a) expected deflection ratio by varying the interlayer stiffness and (b) typical deformed shape.

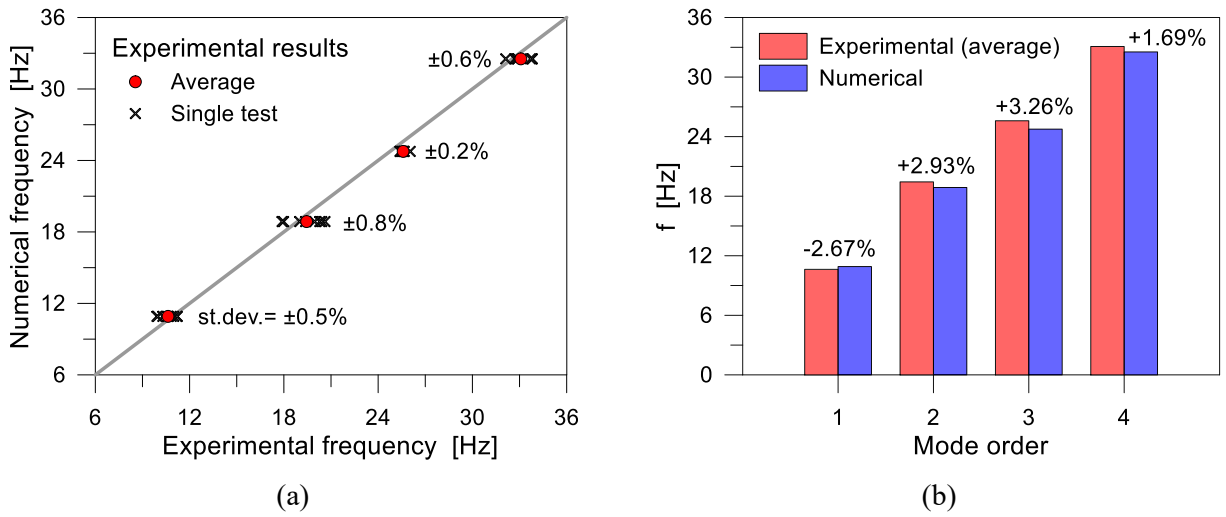

Fig. 8. Comparison of experimental and numerical vibration frequencies: (a) all experimental data (with standard deviation) and (b) average results (with percentage scatter).

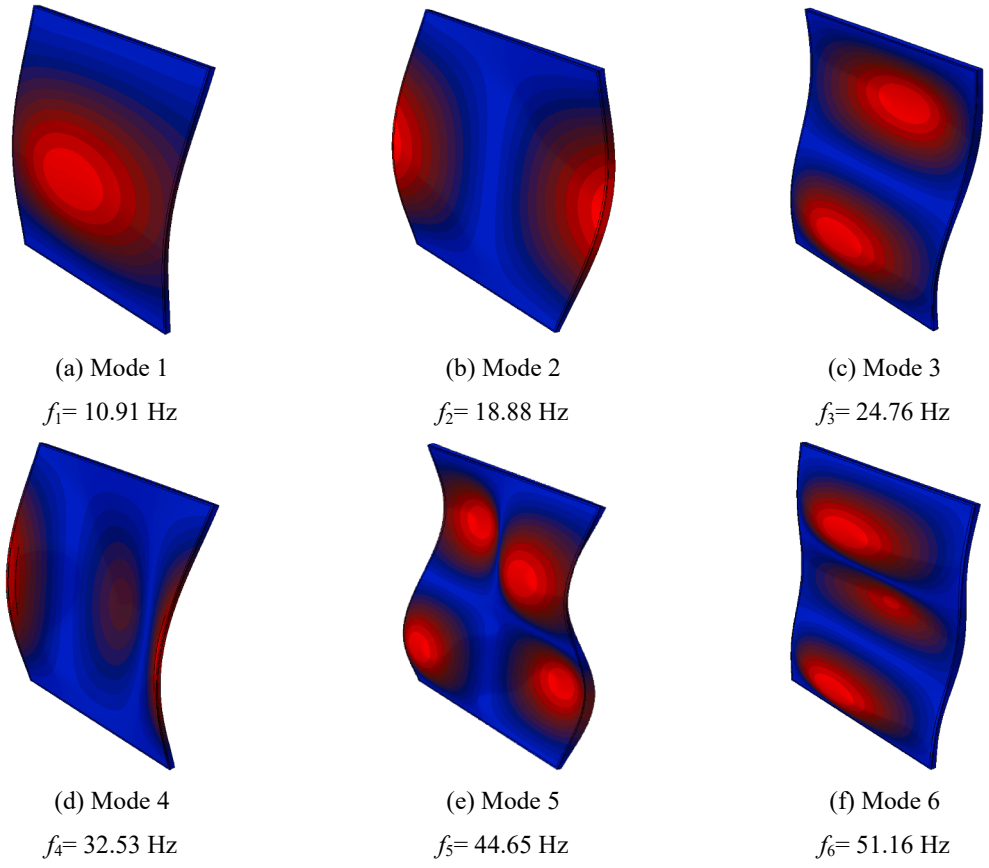

Fig. 9. Numerical vibration modes of the PV module arranged as in the experimental setup.

vibration frequencies is in the range of ± 0.061 Hz for the fundamental mode, ±0.027 Hz for the second, ±0.024 Hz for the third and ± 0.014 Hz for the fourth vibration mode (Fig. 11 (b)). Overall, the predicted results are mostly in line with the "full" estimates, which represent the top limit condition for the system. This is not the case for the PV module as in the limit "abs" configuration, where major effects due to the weak shear bond take the form of a relatively low vibration frequency (Fig. 11 (a)) and a standard deviation from average value up to ± 0.8 Hz (Fig. 11 (b)).

Overall, the parametric results in Fig. 8 confirm that – disregarding the shear bond efficiency – the low vibration modes of the PV module are well separated and slightly affected (in terms of frequency) by the final installation layout, as far as the position of brackets is kept fix.

5.2.3. *Interlayer stiffness*

The parametric analysis was successively extended to assess the effect of a progressive modification of the interlayer stiffness. For the purpose of present study, the elastic modulus E_{int} in Table 1 was

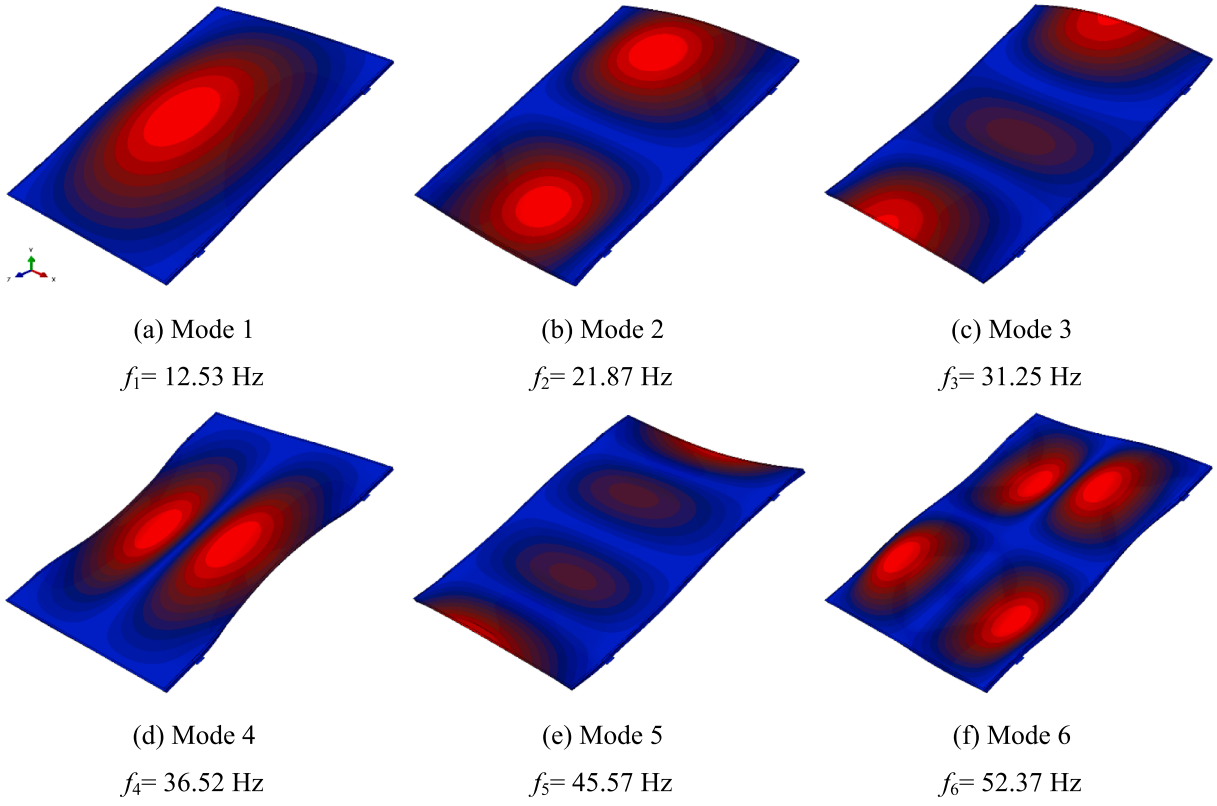

Fig. 10. Reference vibration modes of the PV module restrained by four brackets (α = 40°).

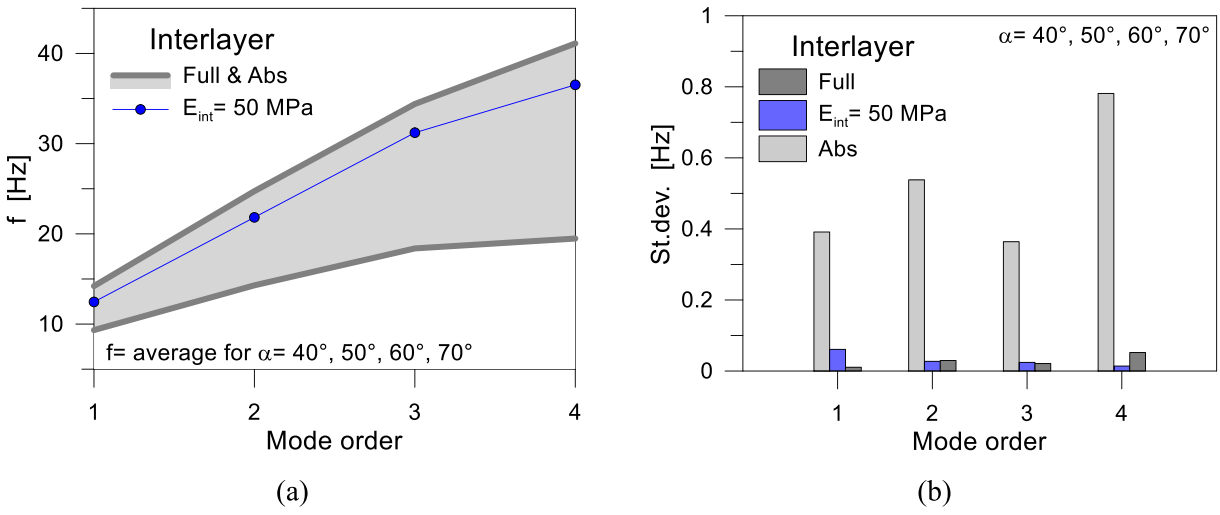

Fig. 11. Vibration modes of the PV module as a function of α: (a) frequency and (b) standard deviation from average frequency.

progressively modified in the range from 0.1 MPa up to 70 GPa, which correspond respectively to the "abs" lower limit and to the ideal "full" configuration in which the interlayer has the same rigidity of the glass front cover.

In terms of vibration modes and shapes of the PV module, no marked modifications were noted compared to Fig. 10. Besides, a major effect of interlayer stiffness was numerically quantified in the modification of vibration frequencies for the examined PV module. In this regard, the typical results can be seen in Fig. 12 (a) to (d) in terms of frequency trend as a function of E_{int}, for the four lower vibration modes, which are characterized (according to Fig. 10 (a) to (d)) by one-to-three half sinewaves for the PV module.

As far as E_{int} ideally increases, the corresponding vibration frequency progressively increases for all the detected vibration modes.

Most importantly, Fig. 13 further emphasize the interlayer effect on the vibration frequency, as a function of the "abs" or "reference" (Table 1) hear bonding level offered by the interlayer.

Compared to a weak bond in Fig. 13 (a), it can be seen that the minimum contribution offered by the interlayer cam manifest in a major stiffening contribution for the sandwich section. The calculated percentage scatter of frequency increases tends to increase with the increase of mode order, that is the number of sinewaves and the bending deformation of the system.

Besides, especially for health monitoring purposes, the percentage

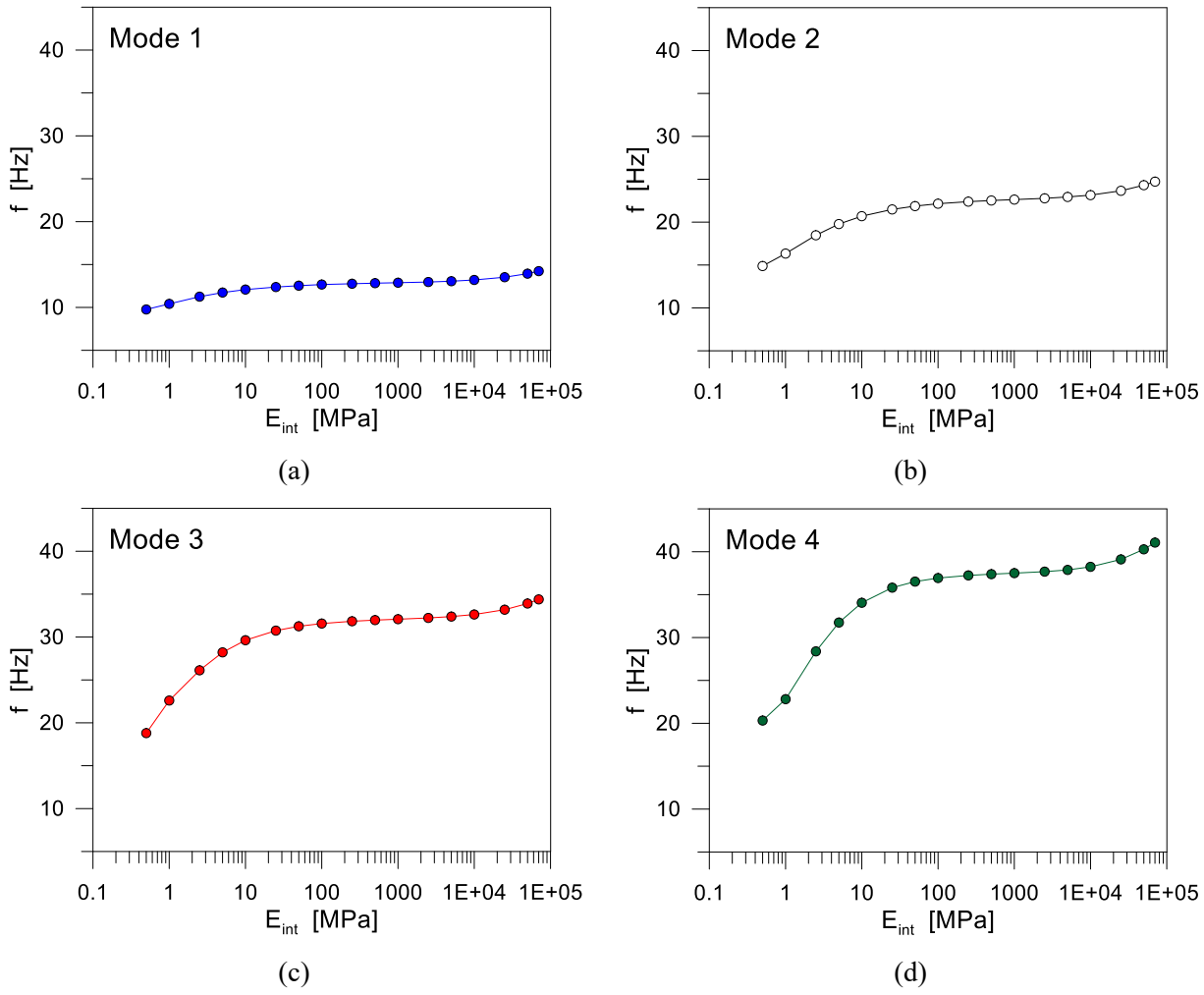

Fig. 12. Vibration frequency of the PV module as a function of E_{int} ($\alpha = 40°$): (a) mode 1, (b) mode 2, (c) mode 3, and (d) mode 4.

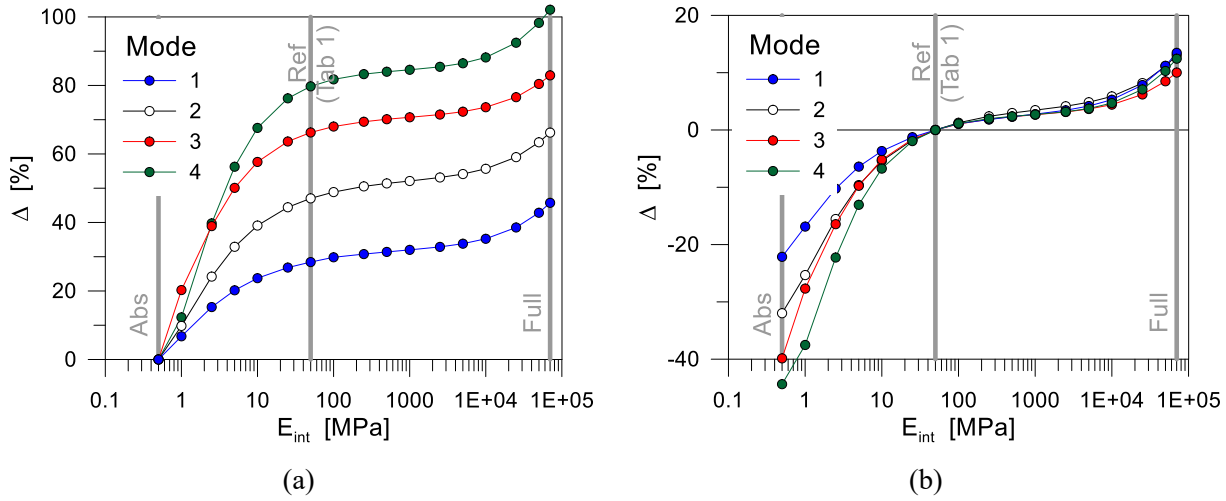

Fig. 13. Percentage variation of vibration frequency of the PV module as a function of E_{int} ($\alpha = 40°$) for modes 1, 2, 3 and 4, based on: (a) "abs" limit and (b) "Ref" value.

frequency variation can be further interestingly measured as a function of the "initial" configuration of the PV module, that is the system with efficient bonding connection at the time of its installation. For the present study, the numerical results in Fig. 13 (b) are calculated in percentage scatter compared to the E_{int} properties reported in Table 1. It can be thus noted that even a major increase in the stiffness of interlayer (i.e., as a function, for example, of high dynamic or impulsive loads), there is no marked modification in the corresponding vibration

frequency. Only for very rigid (but not realistic) bonds, it can be expected a frequency increase up to 13–15 % for the three lower vibration modes of the system. It is worth to note in Fig. 13 (b) that event relatively stiff bonds (i.e., up to ≈1000 MPa in modulus) would result in a minimum increase of stiffness and frequency (less than 3 %). This suggests that the sandwich system under high strain rate effects (i.e., for the PV module under impact loading) cannot take advantage of possible stiffening effects in the interlayer.

It is indeed of major interest the effect of bond rigidity when degrading phenomena, as well as the progressive ageing of interlayer stiffness or even possible delamination of interfaces, can take place in the long-term period. Fig. 13 (b) highlights in fact a frequency decrease down to −40 % when the shear bonding efficiency of the bonding connection tend to vanish ($E_{int} \approx 1$ MPa). In particular, the higher is the mode order for the examined PV system, and the higher is the estimated percentage variation of vibration frequency. As such, at least a frequency decrease in the order of −20 % can be expected for the first vibration mode (Fig. 13 (b)).

In general words, the present analysis confirms that the interlayers have – as in typical glass and composite laminates applications – a key role for the determination of the load-bearing capacity and mechanical performance of typical thin sandwich sections in use for commercial PV modules. In the long-term period, or even in unfavourable environments that could affect the interlayer efficiency, it can be useful to track and detect possible modifications in the mechanical properties of basic components, and thus prevent possible weaknesses or loss or functionalities for PV modules.

5.2.4. *Delamination and non-uniform degradation of interlayer*

The parametric study finally extended to assess possible effects due to scattered delamination of EVA films from the sandwich components, as well as possible non-uniform material softening and decrease in stiffness (such as in presence of severe temperature spots in the PV module). To this aim, a set of numerical analyses was carried out for the FE model as in Table 1, by imposing a set of random configurations characterized by localized delamination / damage. This effect was taken into account by considering different degraded areas (compared to the full bonding area, in percentage terms), and different random patterns (five) for each one of them. Typical examples are shown in Fig. 14, where the red regions represent the mesh elements characterized by a sandwich section with EVA film associated to null shear stiffness. The selected scenarios in Fig. 14 (a) to (c) correspond to 10 % of delaminated encapsulant, 30 % and 50 % respectively. To note that the such a kind of possible delamination or non-uniform rigidity loss is considered – for the present analysis – in terms of EVA material properties only, and does not affect the material features of the encapsulated solar cells (Fig. 14 (d)). This means that the present analysis is carried out to support some possible monitoring steps to perform before any kind of additional fault or crack / failure can affect also the other sandwich components (i.e., glass fracture, cracks in solar cells or interconnects, etc.).

The numerical results from three different damage extensions (10, 30, 50 %) and five random configurations for each one of them are proposed in Fig. 15, in terms of percentage variation of frequency for the low vibration modes of the examined PV module.

The trend of results in Fig. 15 shows that the random distribution of possible degraded regions can have some important influence on the expected vibration frequency of the examined PV modules, and thus on the overall load-bearing capacities. Besides, no modification in mode order can be noted (Fig. 10). Also, the percentage decrease of the estimated vibration frequencies in Fig. 15 is generally higher for increasing mode order. More in detail, when the stiffness reduction covers the 10 % random bonding area, see Fig. 15 (a), the frequency decrease is generally small, around −0.5 % for the presently considered values. When the frequency reduction compared to the initial stage is about ≈2% or higher, this kind of evidence can be indeed associated to major debonding or scattered damage /stiffness decrease for the encapsulant layers, and should be thus carefully taken into account (see Fig. 15 (b) and (c)).

5.2.5. *Hot spotting*

In terms of possible faults in PV modules, in conclusion, final efforts were spent for the frequency sensitivity in terms of early hot spot detection, where various thermal, infrared and sensor-based monitoring solutions are addressed in the literature [4–7]. In this regard, the attention was mostly addressed on preliminary considerations about the effects of cell-based hot spotting, rather than string-based one [55]. The reference FE model was further adapted to take into account a selection of simplified (but realistic) hot spot configurations. As an example, the

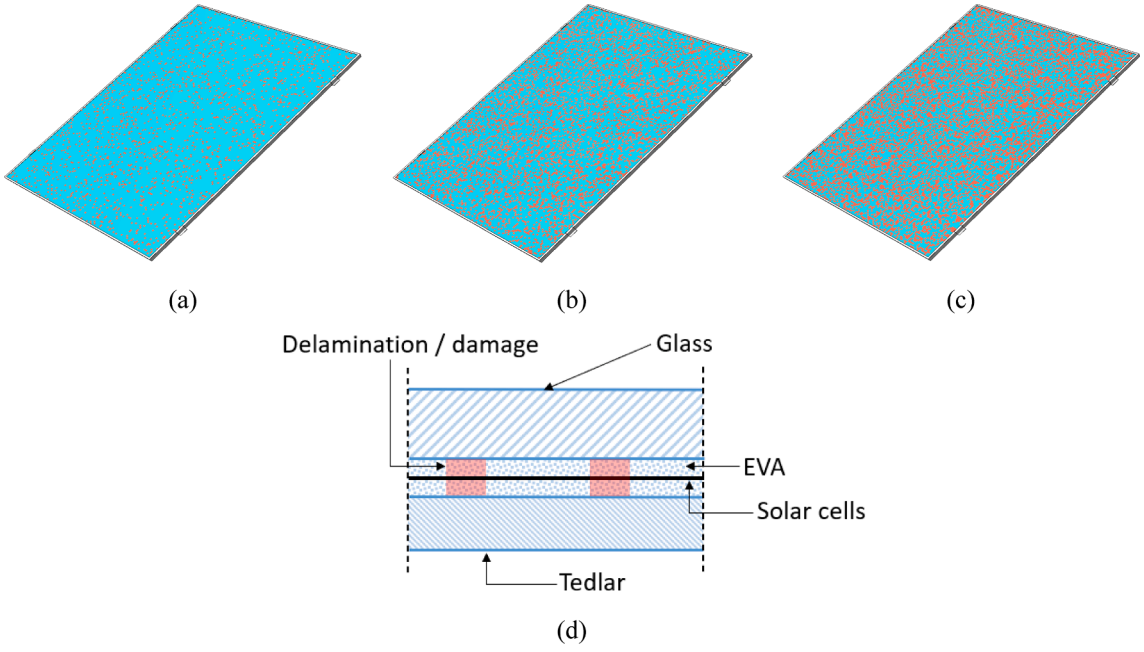

Fig. 14. Numerical analysis of vibration frequency sensitivity to possible delamination / damage (α = 40°): (a) 10 % of delaminated interlayer, (b) 30 % and (c) 50 % (in red), with (d) schematic cross-section.

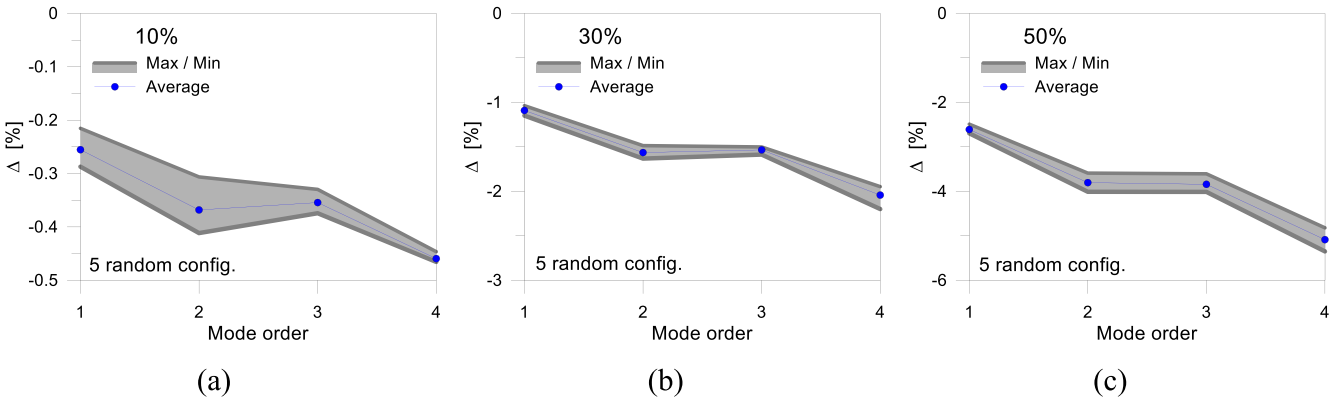

(a) (b) (c)

Fig. 15. Percentage vibration frequency variation due to possible delamination or non-uniform degradation / stiffness reduction (α = 40°): (a) 10 %, (b) 30 % and (c) 50 %, according to Fig. 14.

setup like in Fig. 16 (a) was numerically reproduced in the FE model of Fig. 5, by reducing the mechanical properties of EVA films.

The comparative results of parametric study highlights that the initial temperature rise and localized peak in a single solar cell has generally limited effects on the dynamic features of PV module as a whole, and thus also in terms of vibration frequencies (and modes) associated to the low modes. As shown in Fig. 16 (b) for the "hot spot" curve, the typical percentage reduction of frequency values – compared to the "intact" PV module – was quantified in less than −0.5 % for the examined system. The localized hot spot fault in a single cell can indeed magnify the effects of material deterioration, as it can be seen in Fig. 16 (b) by considering the superimposed effects of non-uniform EVA degradation or debond (like in Section 5.2.4) and combined hot spotting. As shown, the frequency decrease is in this case in the order of −5%, and this suggests that a prompt detection of anomalies (i.e., before any major damage develops further) can be possibly carried out by the present non-destructive methodology. Besides, further investigations are required in this direction, especially to consider different arrangements and extensions of faults (i.e., multiple cells) for the realistic early-stage detection of hot spots.

5.2.6. *Future developments*

The present investigation highlighted the high sensitivity of dynamic features for commercial PV modules (especially the vibration frequency of low modes) to the mechanical properties of interlayers that are used to encapsulate the solar cells and offer the mechanical bond to the sandwich components.

The comparative results of the numerical parametric analysis, in particular, were focused on the percentage frequency decrease, and this was parametrically shown to be relevant (and thus efficiently tracked and monitored) even without visual evidences of major damage in the PV modules. This result implicitly confirms that unfavourable environments, cyclical thermal gradients and long-term phenomena have implicitly severe effects on the mechanical performance of PV modules, even under ordinary loads. Similarly, the early-prompt detection of any anomaly and modification could avoid the progressive fault of PV modules.

The present methodology based on frequency change analysis could be used to monitor, i.e., at selected time intervals, any possible progressive deterioration aspect that could affect the performance of the PV modules as a whole, even without any clear visual appearance, and thus prevent unfavourable stress peaks in the sandwich components but also premature losses of functionality. Further efforts, in this regard, will be spent to assess additional relevant dynamic / mechanic parameters, as well as to experimentally confirm the present numerical outcomes, for a set of different PV module configurations and full-scale samples exposed to real severe environments.

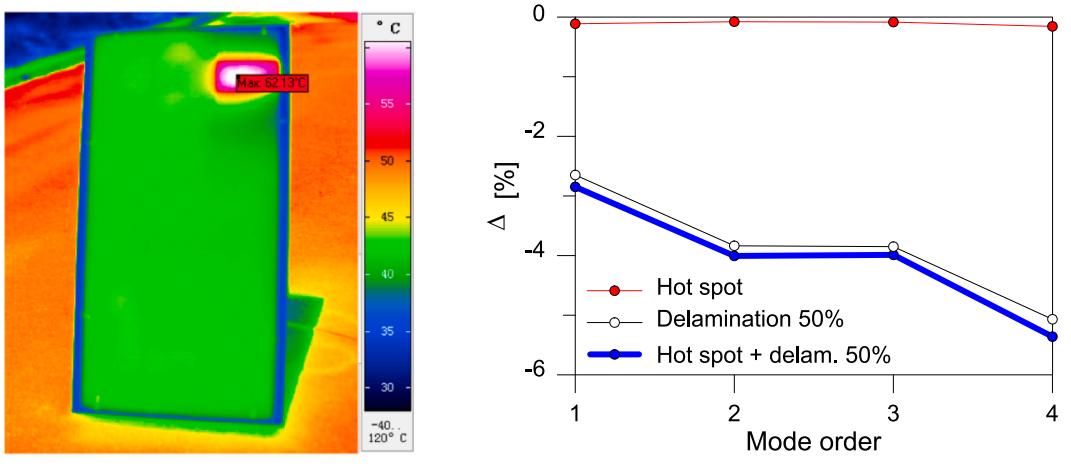

(a) (b)

Fig. 16. Frequency sensitivity to host spot fault: (a) example (reproduced from [7] under the terms and conditions of a CC-BY license agreement) and (b) percentage variation of vibration frequency, based on numerical analysis.

6. Conclusions

Photovoltaic (PV) modules, that are designed to ensure about 20–25 years of functionality, are typically exposed to variable environment scenarios and even unfavourable operational conditions, including the effect of temperature changes, wind, rain, hail and snow, etc. Their mechanical efficiency and performance, in this regard, represents a critical aspect to support an optimal durability and electrical efficiency of PV modules.

Besides, typical sandwich sections are composed of relatively thin top/bottom covers and an interposed film to encapsulate the solar cells. From a mechanical point of view, the interlayers have a key role in ensuring the shear bond between the constituent components, and thus maximize the load-bearing performance capacity of the system. Among others, moreover, the bonding interlayers can suffer for stiffness modification which has direct effects on the composite action and response of the sandwich section.

The present investigation, in this regard, was focused on the frequency assessment to monitor and alert possible major modifications in the encapsulant layers, to prevent major stress peaks and possible severe damage conditions in the sandwich section. A set of parametric numerical analyses was presented, based on preliminary experimental validation, to study the vibration modes and frequencies of a typical commercial PV module, by taking into account the most important boundary conditions of technical interest. The numerical study proved that the vibration frequency can be largely sensitive to possible stiffness modifications in the interlayers, with frequency variations down to −20 % (and even −40 %) when the shear bond efficiency tends to vanish. This suggests that the frequency itself should be usefully checked to reveal the progressive mechanical deterioration or even capture possible defects in the sandwich components. To this aim, the present numerical analysis will be further exploited by including in the investigation a number of different PV module configurations, as well as experimental observations from in-field measurements on aged PV samples.

CRediT authorship contribution statement

Chiara Bedon: Writing – original draft, Software, Investigation, Formal analysis, Conceptualization. **Alessandro Massi Pavan:** Writing – original draft, Validation.

Declaration of competing interest

The authors declare that they have no known competing financial interests or personal relationships that could have appeared to influence the work reported in this paper.

Data availability

Data will be made available on request.

References

[1] A. Mellit, G.M. Tina, S.A. Kalogirou, Fault detection and diagnosis methods for photovoltaic systems: a review, Renew. Sustain. Energy Rev. 91 (2018) 1–17.

[2] Y. Li, K. Ding, J. Zhang, F. Chen, X. Chen, J. Wu, A fault diagnosis method for photovoltaic arrays based on fault parameters identification, Renew. Energy 143 (2019) 52–63.

[3] A. Mellit, M. Benghanem, S.A. Kalogirou, A. Massi Pavan, An embedded system for remote monitoring and fault diagnosis of photovoltaic arrays using machine learning and the internet of things, Renew. Energy 208 (2023) 399–408.

[4] J.A. Tsanakas, P. Botsaris, On the detection of hot spots in operating photovoltaic arrays through thermal image analysis and a simulation model, Mater. Eval. 4 (2013) 457–465.

[5] Z. Zhang, L. Shan, L. Wang, J. Wu, P. Quan, M. Jiang, Study on case analysis and effect factors of hot spot fault for photovoltaic module, Acta Energiae Sol. Sin. 1 (2017) 271–278.

[6] L. Jiang, J. Su, Y. Shi, J. Lai, H. Wang, Hot spots detection of operating PV arrays through IR thermal image, Acta Energiae Sol. Sin. 8 (2020) 180–184.

[7] G. Li, F. Wang, F. Feng, B. Wei, Hot spot detection of photovoltaic module based on distributed fiber bragg grating sensor, Sensors 22 (2022) 4951, https://doi.org/10.3390/s22134951.

[8] M. Sander, S. Dietrich, M. Pander, M. Ebert, J. Bagdahn, Systematic investigation of cracks in encapsulated solar cells after mechanical loading, Sol. Energy Mater. Sol. Cells 111 (2013) 82–89.

[9] S. Dietrich, M. Pander, M. Sander, M. Ebert, Mechanical investigations on metallization layouts of solar cells with respect to module reliability, Energy Procedia 38 (2013) 488–497.

[10] A. Dadaniya, N. Varma Datla, Degradation prediction of encapsulant-glass adhesion in the photovoltaic module under outdoor and accelerated exposures, Sol. Energy 208 (2020) 419–429.

[11] T. Dobra, D. Vollprecht, R. Pomberger, Thermal delamination of end-of-life crystalline silicon photovoltaic modules, Waste Manag. Res. 40 (1) (2022) 96–103, https://doi.org/10.1177/0734242X211038184.

[12] Y. Sangpongsanont, S. Chuangchote, D. Chenvidhya, K. Kirtikara, Annual expansion in delamination of front encapsulant in tropical climate Field-Operated PV modules, Sol. Energy 262 (2023) 111850.

[13] R. Meena, A. Pareek, R. Gupta, A comprehensive review on interfacial delamination in photovoltaic modules, Renew. Sustain. Energy Rev. 189, Part A, 113944 (2024), https://doi.org/10.1016/j.rser.2023.113944.

[14] M.U. Siddiqui, A.F.M. Arif, L. Kelley, S. Dubowsky, Three-dimensional thermal modeling of a photovoltaic module under varying conditions, Sol. Energy 86 (9) (2012) 2620–2631.

[15] M. Jaszczur, Q. Hassan, J. Teneta, E. Majewska, M. Zych, An analysis of temperature distribution in solar photovoltaic module under various environmental conditions, MATEC Web of Conferences 240 (2018) 04004, https://doi.org/10.1051/matecconf/201824004004.

[16] D. Atsu, A. Dhaundiyal, Effect of ambient parameters on the temperature distribution of photovoltaic (PV) modules, Resources 8 (2019) 107.

[17] N. Dabaghzadeh, M. Eslami, Temperature distribution in a photovoltaic module at various mounting and wind conditions: a complete CFD modelling, Journal of Renewable Sustainable Energy 11 (2019) 053503.

[18] Y. Li, L. Xie, T. Zhang, Y. Wu, Y. Sun, Z. Ni, J. Zhang, B. He, P. Zhao, Mechanical analysis of photovoltaic panels with various boundary condition, Renew. Energy 145 (2020) 242–260.

[19] J.Y. Hartley, M. Owen-Bellini, T. Truman, A. Maes, E. Elce, A. Ward, T. Khraishi, S. A. Roberts, Effects of Photovoltaic module materials and design on module deformation under load, IEEE J. Photovoltaics 10 (3) (2020) 838–843.

[20] M. Corrado, A. Infuso, M. Paggi, Simulated hail impacts on flexible photovoltaic laminates: testing and modelling, Meccanica 52 (2017) 1425–1439.

[21] S. Chakraborty, A. Kumar Haldkar, N.M. Kumar, Analysis of the hail impacts on the performance of commercially available photovoltaic modules of varying front glass thickness, Renew. Energy 203 (2023) 345–356.

[22] O. Hasan, A.F.M. Arif, M.U. Siddiqui (2012). Finite Element modeling and analysis of photovoltaic modules. Proceedings of IMMECE12 – 2012 ASME International Mechanical Engineering Congress and Exposition, November 9-15, Houston, Texas, USA.

[23] M. Haghi, M. Aßmus, K. Naumenko, H. Altenbach, Mechanical models and finite-element approaches for the structural analysis of photovoltaic composite structures: a comparative study, Mech. Compos. Mater. 54 (2018) 415–430.

[24] M. Aßmus, S. Bergmann, K. Naumenko, H. Altenbach, Mechanical behaviour of photovoltaic composite structures: a parameter study on the influence of geometric dimensions and material properties under static loading, Compos. Commun. 5 (2017) 23–26.

[25] T. Serafinavičius, P.J. Lebet, C. Louter, T. Lenkimas, A. Kuranovas, Long-term laminated glass four point bending test with PVB, EVA and SG interlayers at different temperatures, Procedia Eng. 57 (2013) 996–1004.

[26] L. Andreozzi, S. Briccoli Bati, M. Fagone, G. Ranocchiai, F. Zulli, Weathering action on thermo-viscoelastic properties of polymer interlayers for laminated glass, Constr. Build. Mater. 98 (2015) 757–766.

[27] D. Antolinc (2020). Three-Point Bending Test of Laminated Glass With PVB and EVA Interlayers at Elevated Temperature. Proceedings of Challenging Glass 7 - Conference on Architectural and Structural Applications of Glass. Belis, Bos & Louter (Eds.), Ghent University, Belgium. ISBN 978-94-6366-296-3, doi: 10.7480/cgc.7.4491.

[28] S. Bornemann, S. Henning, K. Naumenko, M. Pander, N. Thavayogarajah, M. Würkner, Strength analysis of laminated glass / EVA interfaces: microstructure, peel force and energy of adhesion, Compos. Struct. 297 (2022) 115940.

[29] J.T. Knight, A.A. El-Sisi, A.H. Elbelbisi, M. Newberry, H.A. Salim, Mechanical behavior of laminated glass polymer interlayer subjected to environmental effects, Polymers 14 (2022) 5113, https://doi.org/10.3390/polym14235113.

[30] K. Naumenko, V.A. Eremeyev, A layer-wise theory for laminated glass and photovoltaic panels, Compos. Struct. 112 (2014) 283–291.

[31] M. Martin, X. Centelles, A. Solé, C. Barreneche, A.I. Fernández, Polymeric interlayer materials for laminated glass: a review, Constr. Build. Mater. 230 (2019) 116897.

[32] S. Dietrich, M. Pander, M. Sander, S.-H. Schulze, M. Ebert (2010). Mechanical and Thermo-Mechanical Assessment of Encapsulated Solar Cells by Finite-Element-Simulation. Proceedings of SPIE – The International Society for Optical Engineering – Reliability of Photovoltaic Cells, Modules, Components, and Systems III, San Diego, California, USA; volume 7773, id: 77730F, doi: 10.1117/12.860661.

[33] M. Paggi, A. Sapora, An accurate thermoviscoelastic rheological model for ethylene vinyl acetate based on fractional calculus, Int. J. Photoenergy 2015 (2015) 252740, https://doi.org/10.1155/2015/252740.

[34] M. Pander, S. Dietrich, S.-H. Schulze, U. Eitner, M. Ebert (2011). Thermo-mechanical assessment of solar cell displacement with respect to the viscoelastic behaviour of the encapsulant. Proceedings of the12th International Conference on Thermal, Mechanical & Multi-Physics Simulation and Experiments in Microelectronics and Microsystems, Linz, Austria, doi: 10.1109/ESIME.2011.5765831.
[35] C. Bedon, F.A. Santos, M. Fasan, Mechanical analysis of the quasi-static and dynamic composite action in PV modules with viscoelastic encapsulant, Materials 2024 (17) (2024) 1317, https://doi.org/10.3390/ma17061317.
[36] M.P. Limongelli, E. Manoach, S. Quqa, P.F. Giordano, B. Bhowmik, V. Pakrashi, A. Cigada, Vibration Response-Based Damage Detection. Structural Health Monitoring Damage Detection Systems for Aerospace, Springer Aerospace Technology:, Cham, Switzerland, 2021.
[37] C. Bedon, S. Noè, M. Fasan, C. Amadio, Role of in-field experimental diagnostic analysis for the derivation of residual capacity indexes in existing pedestrian glass systems, Buildings 13 (2023) 754.
[38] A.D. Dimarogonas, Vibration of cracked structures: a state of the art review, Eng. Fract. Mech. 55 (1996) 831–857.
[39] C. Bedon, Diagnostic analysis and dynamic identification of a glass suspension footbridge via on-site vibration experiments and FE numerical modelling, Compos. Struct. 216 (2019) 366–378.
[40] C. Bedon, M.V. Santi, M. Fasan, Considerations on efficient procedural steps for seismic capacity assessment and diagnostics of historic structural glass systems, Soil Dyn. Earthq. Eng. 163 (2022) 107562.
[41] C. Bedon, S. Noè, Post-breakage vibration frequency analysis of in-service pedestrian laminated glass modular units, Vibration 4 (2021) 836–852.
[42] C. Bedon, Issues on the vibration analysis of in-service laminated glass structures: analytical, experimental and numerical investigations on delaminated beams, Appl. Sci. 9 (18) (2019) 3928.
[43] C. Bedon, F. Santos, Effects of post-fracture repeated impacts and short-term temperature gradients on monolithic glass elements bonded by safety films, Compos. Struct. 319 (2023) 117166.
[44] C. Bedon, M. Fasan (2023). Post-Fracture Stiffness and Residual Capacity Assessment of Film-Retrofitted Monolithic Glass Elements by Frequency Change. Mathematical Problems in Engineering, vol. 2024, Article ID 8922303, 16 pages, 2024. doi: 10.1155/2024/8922303.
[45] U.J. Udi, M.M. Yussof, K.M. Ayagi, C. Bedon, M.K. Kamarudin, Environmental degradation of structural glass systems: a review of experimental research and main influencing parameters, Ain Shams Eng. J. 14 (5) (2023) 101970.
[46] T. Hána, T. Janda, J. Schmidt, A. Zemanová, M. Šejnoha, M. Eliášová, M. Vokáč, Experimental and numerical study of viscoelastic properties of polymeric interlayers used for laminated glass: determination of material parameters, Materials 12 (2019) 2241, https://doi.org/10.3390/ma12142241.
[47] J. Gong, L. Xie, Y. Li, Z. Ni, Q. Wei, Y. Wu, H. Cheng, Analysis of the impact resistance of photovoltaic panels based on the effective thickness method, J. Renewable Mater. 10 (1) (2021) 33–51.
[48] J. Schmidt, T. Janda, M. Sejnoha, J. Valentin (2017). Experimental determination of visco-elastic properties of laminated glass interlayer. Proceedings of 23rd International Conference Engineering Mechanics 2017, Svratka, Czech Republic.
[49] CNR-DT 210/2013; Istruzioni Per la Progettazione, L'esecuzione ed il Controllo di Costruzioni con Elementi Strutturali di Vetro. National Research Council of Italy (CNR): Rome, Italy, 2013. (In Italian).
[50] M.A. Gharaibeh, A.M. Obeidat, Vibrations analysis of rectangular plates with clamped corners, Open Eng. 8 (2018) 275–283.
[51] Simulia, Dassault Systémes. ABAQUS Computer Software; Providence, RI, USA.
[52] EN 572–2:2004. Glass in buildings – Basic soda lime silicate glass products. European Committee for Standardization (CEN), Brussels, Belgium.
[53] EN 485-2, Aluminium and Aluminium Alloys – Sheet, Strip and Plate – Part 2: Mechanical Properties. European Committee for Standardization (CEN), Brussels, Belgium.
[54] Tedlar Technical Bulletin (2020). Mechanical properties of Tedlar Films, 6 pages.
[55] M. Dhimish, Thermal impact on the performance ratio of photovoltaic systems: a case study of 8000 photovoltaic installations, Case Studies Therm. Eng. 21 (2020) 100693.